METHODS

Procedure

After informed consent, participants completed clinical diagnostic interviews (e.g., Clinician-Administered PTSD Scale for DSM-5, CAPS-5; Structured Clinical Interview for DSM-IV Dissociative Disorders), and a battery of self-report measures (e.g., Childhood Trauma Questionnaire, Multidimensional Inventory of Dissociation). After ensuring participants met diagnostic criteria for PTSD with the CAPS-5 interview, they completed neuroimaging procedures. The neuroimaging procedures began with an anatomical scan and then a series of functional scans as detailed in the main manuscript. The order of functional scans was the following: a masked faces task (Gruber, Rogowska & Yurgelun-Todd, 2009), the multi-source interference task (Bush, Shin, Holmes, Rosen, & Vogt, 2003), and a resting state scan. The masked faces task was a block-design task including happy, fearful, and angry faces. All happy, fearful, and angry faces were backwards-masked by a neutral face. The task for the participant was to identify the gender of the neutral face (male vs. female). The multi-source interference task was a block-design, challenging attention task in which the participant was asked to identify the number that was different in a three-digit array (e.g., 100). Trials included control trials in which the target number, that is, the number that was different form the other two, was congruent with its position (e.g., 100), and interference trials in which the target number was incongruent with its position in the array (e.g., 221). During the resting state scan, participants were asked to keep their eyes open (blinking naturally) and to think about nothing in particular.
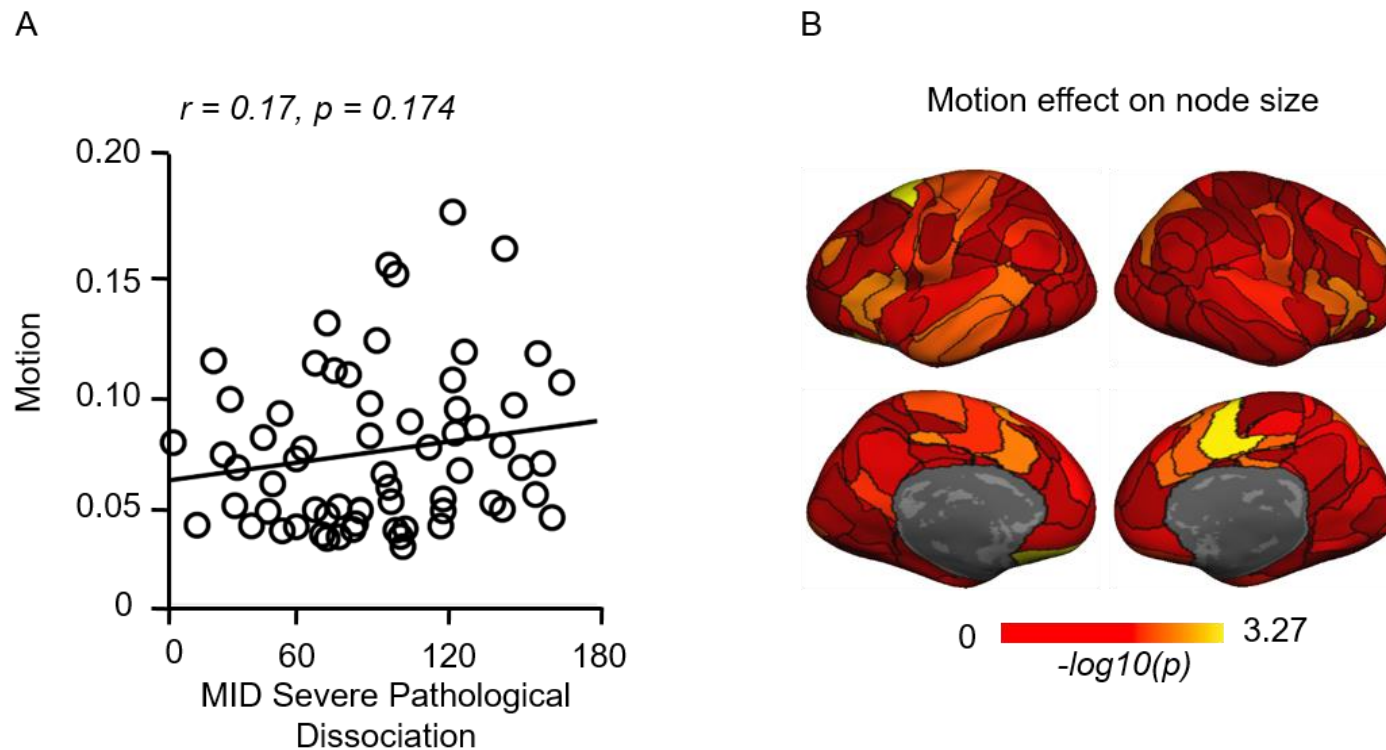
Visualization

All imaging results were visualized on fsaverage 6 using the FreeSurfer. The connectograms demonstrating connections contributing to symptoms estimation (e.g. **Fig. 1**) were created using Circos (http://circos.ca/).

Code availability

Codes can be downloaded from http://nmr.mgh.harvard.edu/bid/DownLoad.html.

FIGURE S1. Head motion effects

A

r = 0.17, p = 0.174

B

Motion effect on node size


0   3.27
-log10(p)

(A) No correlation was found between head motion and severe dissociation scores, $r = 0.17$, $p = 0.174$. A circle in the scatter plot represents each participant. **(B)** No significant correlation was found between motion and node size. The map shows the uncorrected significance values (logarithmic scale) for the correlations between motion and node size. Significance threshold was set $p < 0.05$ after Bonferroni correction, logarithmic scale: -log10 (0.05/92) = 3.27.

FIGURE S2. Covariate effects on connectivity
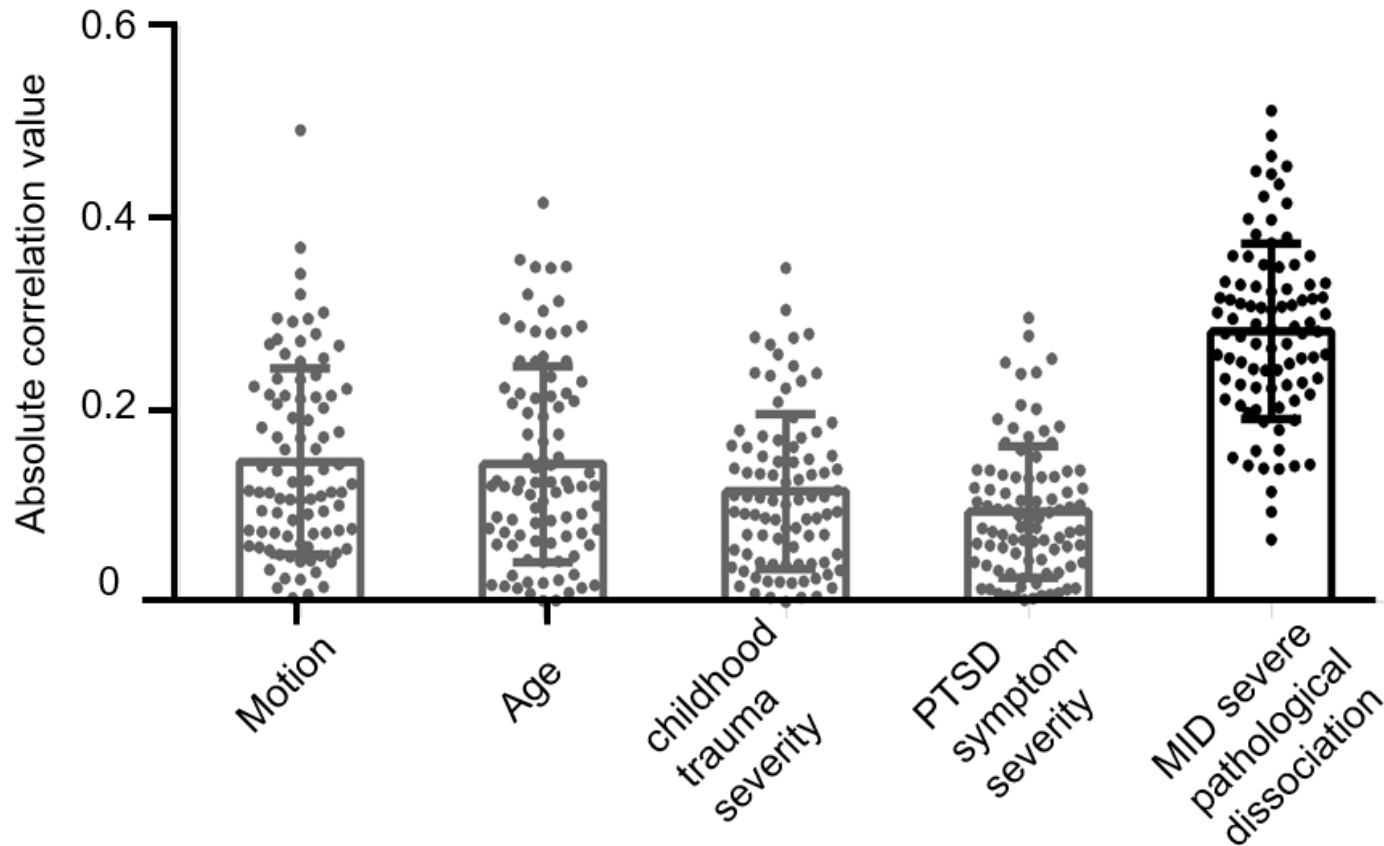

To better understand the contribution of covariate effects compared to the primary dissociation effects, we calculated he Pearson correlations between covariates including motion, age, childhood trauma severity, PTSD symptom severity and the 90 connections identified in the MID severe pathological dissociation prediction model. Covariates (grey bars) were less correlated with the connectivity (mean correlation across 90 connections < 0.15, p< 0.0001, one-way ANOVA test), compared to the correlation between the dissociation score (Black bar) and connectivity (mean correlation across 90 connections = 0.28). Each dot represents one of the 90 connections identified in the MID severe pathological dissociation prediction model.

FIGURE S3. Homologous functional regions across individuals
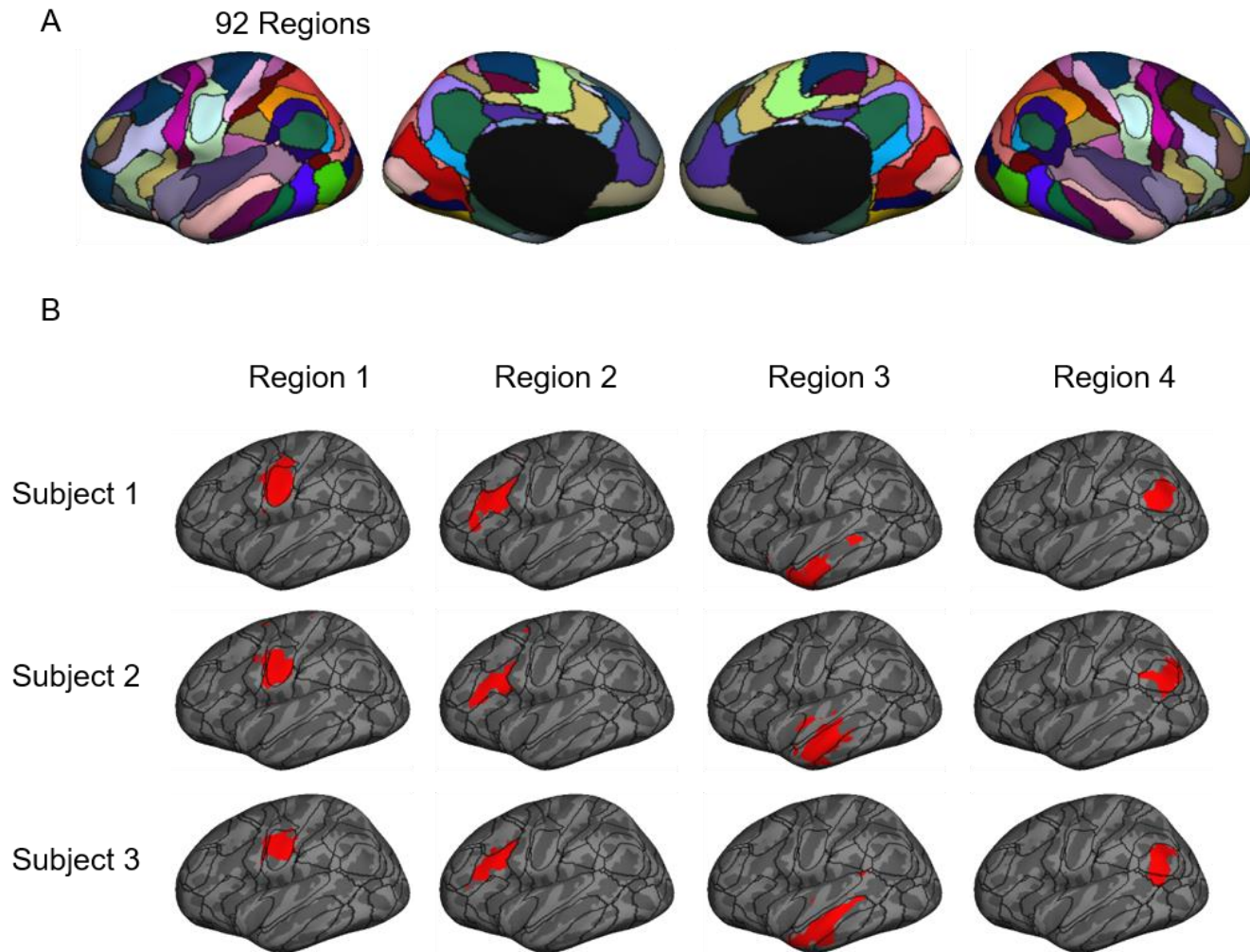
(A) 92 functional ROIs defined in the group-level atlas. (B) Functional ROIs demonstrated substantial inter-individual variability across different participants. Four exemplar ROIs in three randomly selected participants were plotted on the brain surface. The ROIs showed marked variability in size and position. Black lines delineate the 92 atlas ROIs.

FIGURE S4. The severe dissociation scores prediction was mainly driven by between-network connectivity that was more accurately estimated using individually specified ROIs
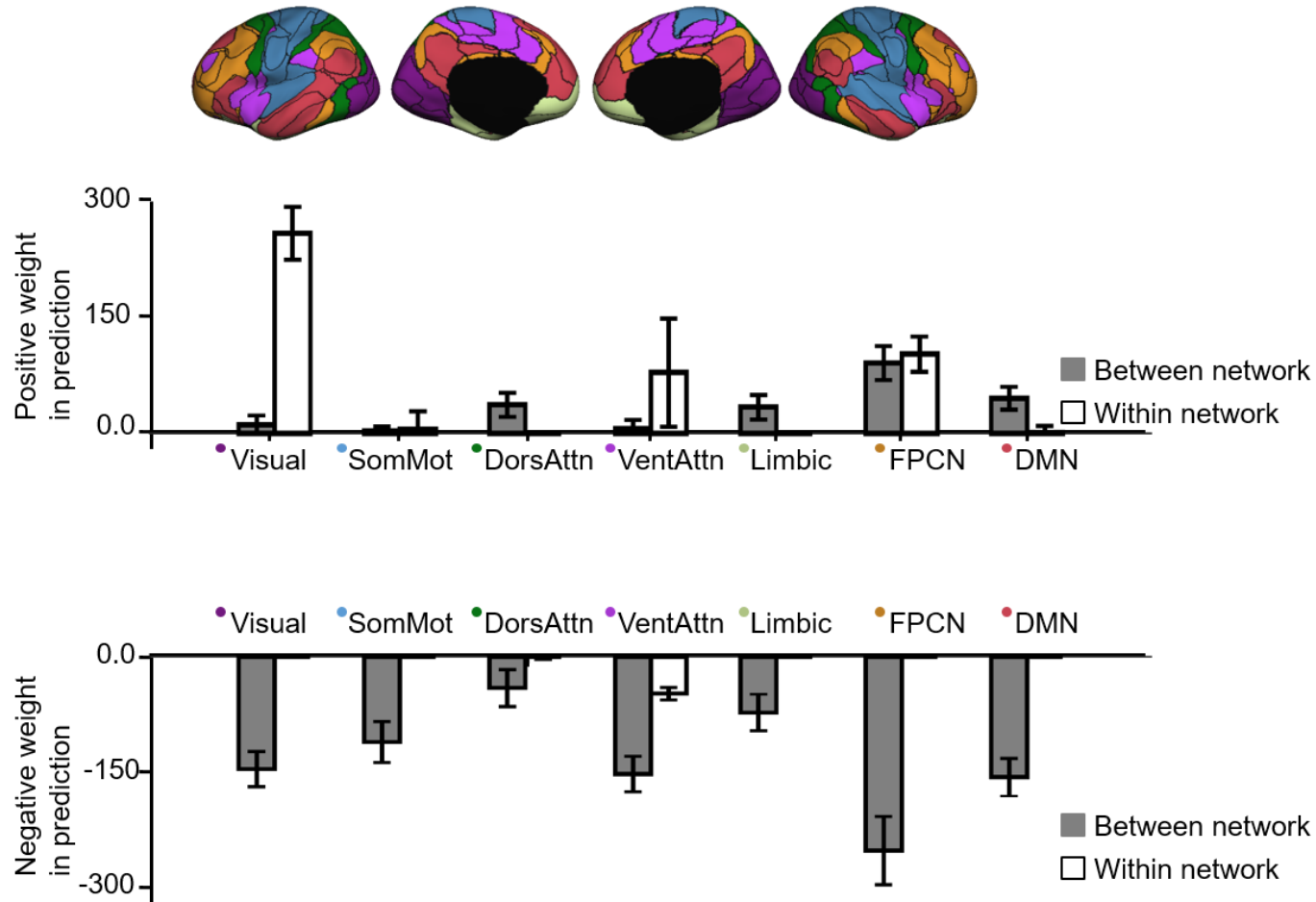
The contributions of between-network connectivity and within-network connectivity in the prediction analyses were quantified for each of the 7 networks based on their positive and negative weights in the prediction model separately. DMN: default mode network; Visual: visual network; SomMot: somatosensorimotor network; DorsAttn: Dorsal attention network; VentAttn: Ventral attention network; FPCN: frontoparietal control network; Limbic: limbic network.

TABLE S1. Prediction performance estimated by different objective indices and cross validations

Prediction performance	r	r^2	Mean squared error
Leave one out cross validation	0.496	0.246	1401.5
5-fold out cross validation	0.366±0.08 range: 0.143 – 0.508	0.13±0.06 range: 0.02 – 0.26	1898.6±242.6 range: 1450.1 – 2540.2

DISCUSSION

Between-Network Connections Drive Symptom Prediction Models

Our individual-based ROI size and functional connection model performed better than atlas-derived ROIs, suggesting these traditional methods for ROI estimation may fail to identify functional connectivity relevant to symptom estimation. This is consistent with recent work from our group and others, indicating that connectivity estimates derived from group-defined functional regions fail to yield symptom prediction models that are both sensitive and specific.

Most likely, this lack of sensitivity and/or specificity using group-based functional regional boundaries is due to several factors, however, precision of between-network correlation strength may be the key factor in our study. That is, our results indicate that connectivity among regions in distinct networks were most predictive of severe dissociation scores ("between network connectivity"), and it seems that regions defined using group-level boundaries do not allow for precise estimates of between-network correlation strength, where the baseline (i.e., normative) connectivity is close to zero and therefore theoretically more subject to noise contamination. While it remains speculative that the individualized regional approach yielded more accurate estimates of between-network connectivity than group-based regions, we view the differential ability to estimate symptoms using the former approach as parsimonious with this interpretation. We have observed similar patterns of between-network connections providing better symptom prediction in our other recent work in obsessive-compulsive disorder and psychotic illness (Brennan et al., 2019; Wang et al., 2018).

References

Brennan BP, Wang D, Li M, Perriello C, Ren J, Elias JA, et al. Use of an Individual-Level Approach to Identify Cortical Connectivity Biomarkers in Obsessive-Compulsive Disorder. Biol Psychiatry Cogn Neurosci Neuroimaging. 2019 Jan;4(1):27–38.

Bush G, Shin LM, Holmes J, Rosen BR, Vogt BA. The Multi-Source Interference Task: validation study with fMRI in individual subjects. Mol Psychiatry. 2003 Jan;8(1):60–70.

Gruber SA, Rogowska J, Yurgelun-Todd DA. Altered affective response in marijuana smokers: an FMRI study. Drug Alcohol Depend. 2009 Nov 1;105(1-2):139–53.

Wang D, Li M, Wang M, Schoeppe F, Ren J, Chen H, et al. Individual-specific functional connectivity markers track dimensional and categorical features of psychotic illness. Mol Psychiatry. 2018 Nov 15; Available from: http://dx.doi.org/10.1038/s41380-018-0276-1